ISSN (Print) 1226-1750
ISSN (Online) 2233-6656
Journal of Magnetics 20(2), 138-147 (2015) http://dx.doi.org/10.4283/JMAG.2015.20.2.138

Nano-scale Inter-lamellar Structure of Metal Powder Composites for High Performance Power Inductor and Motor Applications

Hakkwan Kim and Sung Yong An*

Corporate R&D Institute, Samsung Electro-Mechanics, Gyeonggi-do 443-743, Korea

(Received 11 April 2015, Received in final form 31 May 2015, Accepted 5 June 2015)

The unique nano-scale inter-lamellar microstructure and unparalleled heat treatment process give our developed metal powder composite its outstanding magnetic property for power inductor & motor applications. Compared to the conventional polycrystalline Fe or amorphous Fe-Cr-Si-B alloys, our unique designed inter-lamellar microstructure strongly decreases the intra-particle eddy current loss at high frequencies by blocking the mutual eddy currents. The combination of optimum permeability, magnetic flux and extremely low core loss makes this powder composite suitable for high frequency applications well above 10 MHz. Moreover, it can be also possible to SMC core for high speed motor applications in order to increase the motor efficiency by decreasing the core loss.

Keywords : inter-lamella structure, magnetic composite, power inductor, core-loss, eddy current loss

1. Introduction

Soft magnetic materials are important functional materials widely used in electric, computer and communication fields. During the last several decades, many soft magnetic materials including pure Fe and a series of its alloys [1], soft ferrites [2] and Fe-based amorphous or nanocrystalline alloys [3] have been investigated for magnetic devices. Recently, soft magnetic composites have aroused much scientific interest because these materials exhibit good overall performance with high combined magnetic induction and permeability, low core loss and high working frequency, which are in latent demand for the application of high power inductors, motors and generators.

As is known, although Fe-Si and Fe based amorphous alloys also possess good magnetic properties, these materials still have high loss problems at higher frequency and fast speed motor applications.

For this reason, two main researches have been studied so far to minimize the eddy current loss: inter-particle & intra-particle eddy current loss as depicted in Fig. 1.

Considering the view point of inter-particle eddy current loss, conventional soft magnetic composite prepared by coating Fe based powder with insulating materials have been investigated earlier for low loss applications [4]. Especially, many studies have been focused on the phosphate coated composites [5-7] and it is reported that the phosphate coating can lead to high electrical resistivity and good adhesion, even though its maximum annealing temperature only up to 550°C.

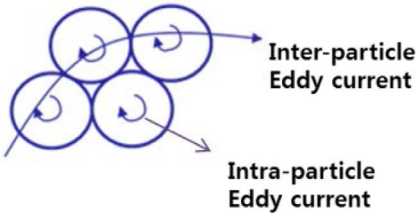

Fig. 1. (Color online) Inter & intra-particle eddy current loss.

Fe based amorphous and nanocrystalline alloys have been also studied strenuously because of their significantly low core loss from the view point of the intra-particle eddy current loss. However, these materials cannot be widely used in high power applications due to their lower magnetization than those of pure Fe or Fe based polycrystalline alloys.

In this study, we fabricated new optimum soft magnetic composites having inter-lamellar structure manufactured by consecutive plasma carburization and heat treatment as shown in Fig. 2. Fe_3C cementite walls with nm scale

*Corresponding author: Tel: +82-31-210-3017
Fax: +82-31-300-7900, e-mail: sung.an@samsung.com

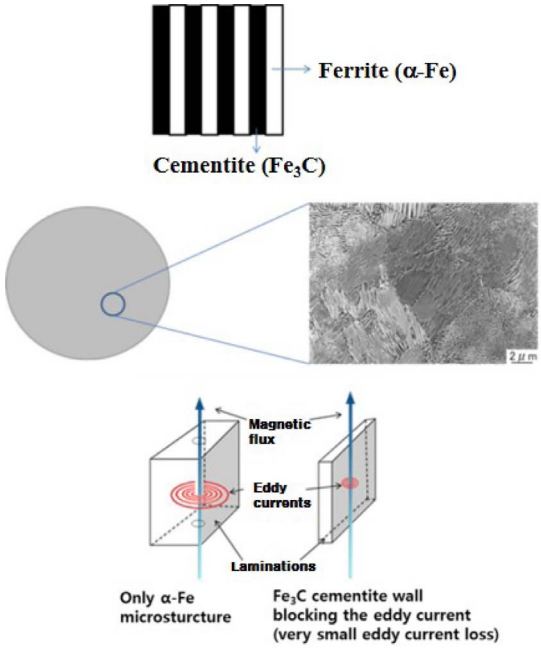

Fig. 2. (Color online) Inter-lamellar structure decreases the eddy current loss.

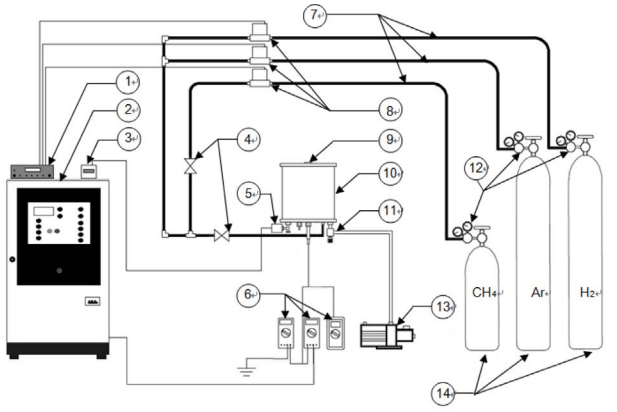

1	Flow controller	8	Flow meters
2	Power supply	9	Preview window
3	Digital display for pressure reading	10	Vacuum chamber
4	Valves	11	Valve for pressure regulation
5	Capacitive manometer	12	Manometers
6	Multi-meters	13	Vacuum pump
7	Piping for gas supply	14	Gas cylinders

Fig. 3. (Color online) Schematic representation of the plasma apparatus employed in this research [8].

thickness function as blocking the eddy currents and results in decreasing the total eddy currents drastically. To the best of our knowledge, there are no reports trying to make successful composites by decreasing the inter & intra-particle eddy current loss simultaneously, also maintaining high magnetization similar to pure Fe, even though this method is quite simple, easy to use and inexpensive compared to the amorphous or nanocrystalline alloys. We will describe the manufacturing process to make this soft magnetic composite, characterize the microstructure in detail, and explain the mechanism how the microstructure changes have an influence on the magnetic property.

Eddy currents flow is blocked by cementite walls.

2. Experimental

2.1. Carburization and consecutive heat treatments

High purity Fe powders, manufactured from KITECH – Korea Institute of Industrial Technology, with an average particle size of 5~10 μm were used as the raw material. The inter-lamellar structure was formed by the consecutive DC-plasma carburization and heat treatments. There are three steps in the preparation of making metal powders having inter-lamellar structure, namely passive and contaminated thin surface film removing, low temperature plasma carburizing, homogenization heat treatment which affect the interval and width of Fe_3C cementite and α-Fe phase of inter-lamellar structure. Low temperature plasma carburizing was carried out in a pulsed plasma reactor with a hot wall chamber as schematically described in Fig. 3. Passive and contaminated thin surface film was removed by a sputtering step conducted at 400°C for 1 hour using high intensity pure hydrogen plasma. Carburizing was conducted at 480°C for 12 hours. A gas mixture composition of H_2, Ar and CH_4 was used. During the heat treatment, the optimum carburizing temperature was measured by two thermocouples attached in the powder compacted mold. The homogenization heat treatment was conducted at 800°C for 2 hours to diffuse carbon into the austenite Fe phase sufficiently and then furnace cooled to room temperature in order to form inter-lamellar structure uniformly within the powder matrix.

2.2. Electrical insulation coating

Fe/SiO_2 soft magnetic composite by coating Fe host particles with amorphous SiO_2 layers with 50 nm thick were fabricated by mechanofusion method as shown in Fig. 4.

Application of mechanical force to a mixture of guest (SiO_2) and host (Fe) particles will form an ordered mixture where guest particles are sufficiently small (~50 nm diameter) as to be held to the surface by van der Waals forces. Further mechanical action can cause these particles to generate a continuous coating in the form of a non-porous film layer to prevent from flowing inter-particle eddy currents. The nature of coating and whether or not a dry coating is achievable through mechanical action is relatively hard to predict and has generally been determined

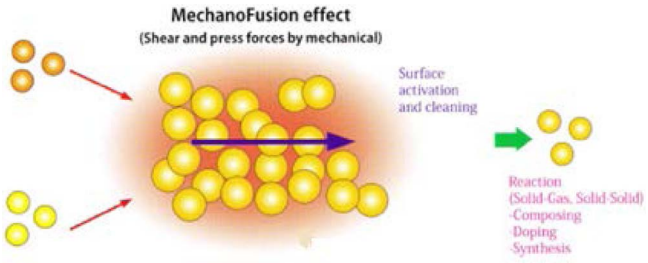

Fig. 4. (Color online) Mechanofusion effects [9].

empirically.

2.3. Microstructure characterization

The method used for measuring inter-lamellar spacing took advantage of the high resolution power of the atomic force microscopy (AFM) technique, allied to the versatility of the image analysis system of the equipment, a Nanoscope III from Digital Instruments. The image analysis system provides a topographic profile of the microstructure along the test line. The system offers the possibility of measuring distances between markers applied to such a profile. Appropriate positioning of these markers allows the measurement of the distances between the center of adjacent cementite or ferrite lamellae or of groups of *n* lamellae. For each selected powder considering the particle size, it was generally possible to apply the test line five to ten times, leading to an average value of the spacing in that selected area. At least 10 areas were analyzed on each metallographic specimen. The sample cross-section was etched with NITAL (an etching solution consisting of ethyl alcohol and nitric acid) so as to be subject to metallographic observation under an optical and electron microscope such as scanning electron microscopy (SEM), transmission electron microscopy (TEM) and scanning transmission electron microscopy (STEM) as well as AFM. Standard preparation techniques such as ultra-microtomy and ion beam etching are not able to provide cross-sectional specimen of particles having acceptable quality. To overcome this bottleneck, we have used a focused ion beam (FIB) microscope for the preparation of cross-sectional TEM specimen. In some cases, a thin Pt layer was locally deposited on the sample to enhance charge and heat transfer and also to prevent the damage of Ga ion bombardment. Related elemental analysis and diffraction patterns were also measured to analyze the composition and phase of constituents.

2.4. Magnetic properties measurement

For the measurement of the alternating current magnetic properties by impedance analyzer and B-H analyzer, toroid samples were obtained by compacting the coated particles with 2.5% epoxy binders under the static pressure of about 300 MPa and annealing at 500°C for 2 hours to relieve the residual stress that can increase the hysteresis loss. The direct-current magnetic properties were also measured on powder and bulk samples, using a vibrating sample magnetometer (VSM 7300 series by Lakeshore Co. Ltd) to obtain the information of magnetization and coercivity.

3. Results and Discussion

3.1. Insulation coating

As shown in Fig. 5, STEM micrograph images and

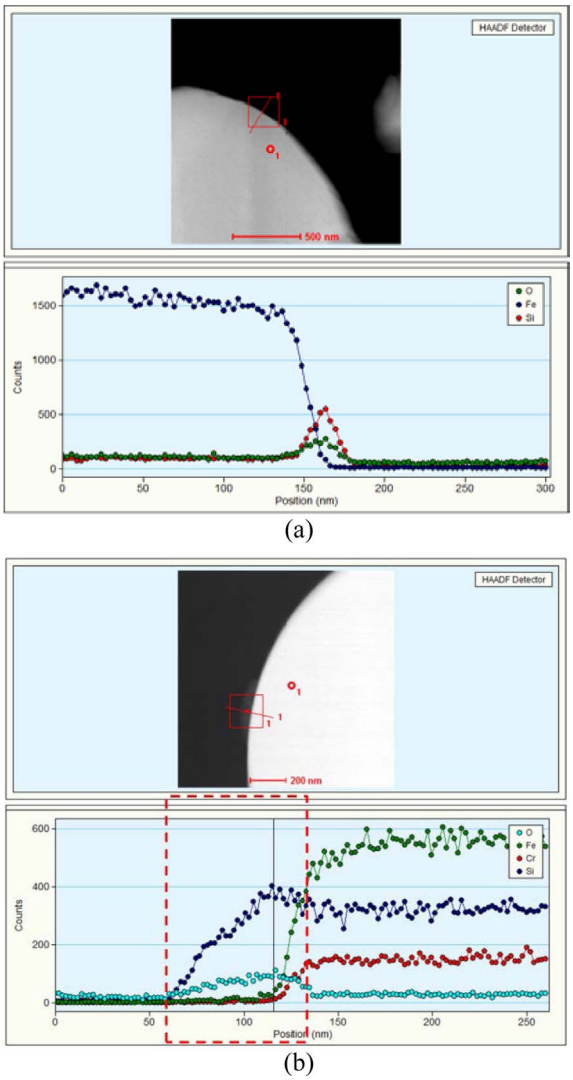

Fig. 5. (Color online) STEM images and related element profiles for SiO_2 insulation coated Fe particles: (a) Fe crystalline and (b) FeCrSiB amorphous particle. Continuous 50 nm scale Si oxide insulation layer is mechano-chemically formed to exclude the effect of inter-particle eddy current loss on the total core loss.

related elements line-scan profiles represent that mechanical action in the mechanofusion method can cause 50 nm scale SiO_2 particles to generate a continuous coating in the form of a non-porous film layer to prevent inter-particle eddy currents. This continuous film layer is about 50 nm thick and composed of Si and oxygen. We could not find any impurity elements that can be typically detected in wet coating or deposition methods, which often cause the inevitable environmental concerns and decrease the magnetic properties. The factors determining the inter-particle eddy current loss include insulation layer composition, which affects the electrical resistivity, and the continuity of coating layer, which can control the amount of eddy current flows. Si oxide is well known for the good insulating materials having 9.24 eV energy band gap [10]. According to the solid state physics, when the band gap energy exceeds ~9 eV, the material can be classified as an insulator because the thermal energy at 300K is clearly insufficient to allow electrons from the valence band to be promoted to the conduction band. In this case, the valence band (and all bands of lower energy) is fully occupied, and the conduction band is empty.

According to these data, we can anticipate that this continuous Si oxide coating layer without defects is capable of minimizing the eddy current flows among particles through particle boundary in the core mass. We can also scrutinize and focus on the relationship between the intra-particle eddy current and microstructure transformation because it is persuasive to separate the intra-particle eddy current loss from the total core loss if insulation layer is completely coated onto the surface of every particle.

3.2. Inter-lamellar microstructure

Carburization and heat-treated Fe powders are prepared to make the inter-lamellar microstructure within the powder core. Non-carburized polycrystalline pure Fe and FeCrSiB amorphous powders are also prepared to compare their microstructure difference and magnetic properties with one another. Pure Fe is mainly used for increasing the DC bias or net magnetic flux due to its high magnetization and Fe amorphous is mainly used for further reduction in core loss.

Fig. 6 shows the typical cross-sectional SEM images of three kinds of powders (non-carburized polycrystalline Fe, FeCrSiB amorphous and carburized polycrystalline Fe) and corresponding elemental analysis results.

Non-carburized Fe powder is composed of 2~3 um scale average grains and has polycrystalline α-ferrite structure. As shown in the EDS results, the carbon contents of this powder are relatively very low compared to the other two powders and this means that it is not enough to

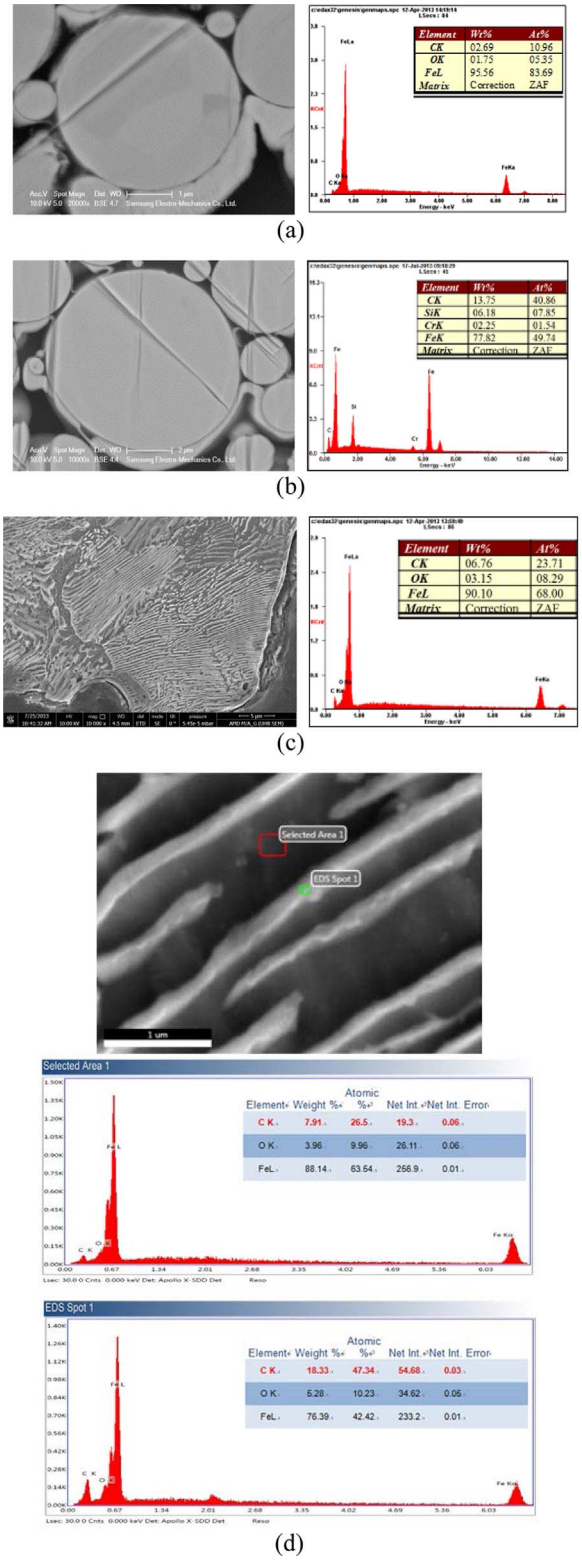

Fig. 6. (Color online) SEM micrographs and corresponding EDS analysis results show that the microstructure difference among (a) pure polycrystalline Fe, (b) amorphous FeCrSiB and (c) carburized and heat-treated Fe. (d) Carburized Fe clearly shows the lamellar structure composed of carbon rich iron carbide phase (bright area) and α-Fe, ferrite phase (gray area).

precipitate iron carbide to make inter-lamellar structure. On the contrary, FeCrSiB amorphous powder has no grain boundaries and low iron contents due to the metalloid elements such as Si, B, Cr and carbon. At high magnification, we observe small crystalline-like phase with about 5~10 nm in diameter, randomly dispersed within the amorphous matrix. Akihiro Makino and his colleagues also found the same small islands and they revealed these are α-ferrite crystalline [11].

In case of carburized and heat-treated Fe powder, two-phase inter-lamellar structure is manifest and comprises alternating layers of α-ferrite and high carbon contents iron carbide as shown in Fig. 6(d). From this trench type inter-lamellar structure, we can surmise that the intra-particle eddy currents flow is obstructed by these regularly formed iron carbide walls.

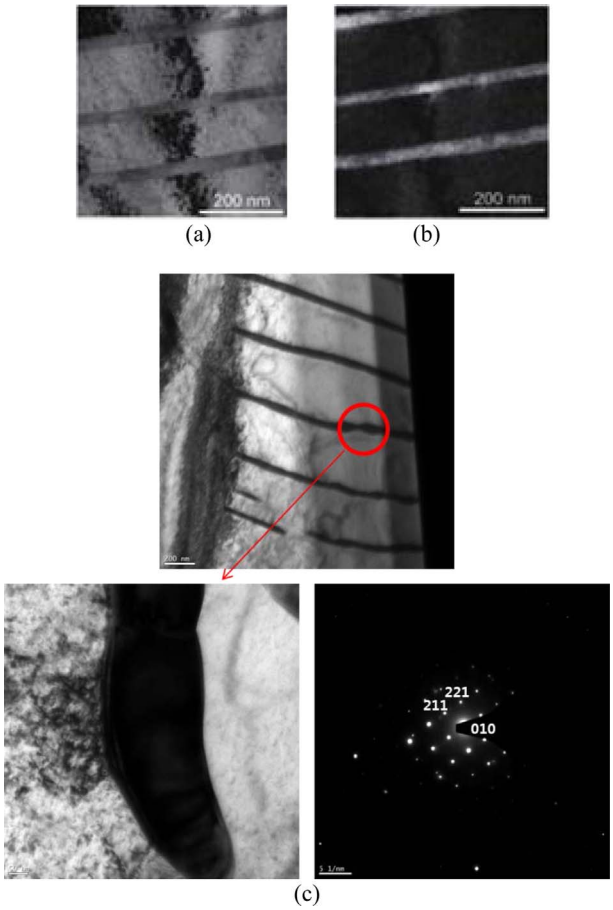

Fig. 7. (Color online) Electron micrographs, corresponding carbon mapping image and SAD pattern of the inter-lamellar microstructure: (a) TEM BF image, (b) Corresponding carbon mapping image in STEM mode shows that the bright area has high carbon contents. (c) Fe carbide BF images and corresponding SAD pattern from the high carbon portion of the inter-lamellar microstructure (black region) reveals that iron carbide is Fe_3C cementite.

The classical metallographic techniques usually applied to the measurement of inter-lamellar spacing were reviewed by Ridley [12], who pointed out that the examination of thin foil specimens or shadowed carbon replicas by transmission electron microscopy (TEM) was the most versatile technique to analyze fine inter-lamellar structure. Moreover, we can also verify the iron carbide is Fe_3C cementite using selected area diffraction (SAD) pattern.

As shown in Fig. 7, the average width of α-ferrite and Fe_3C cementite is about 200~300 nm and 50~100 nm, respectively, even though this measurement is applied to the specific local area due to the TEM sample limitation. They are measured using the TEM bright-field (BF) image and corresponding carbon mapping images. Corresponding

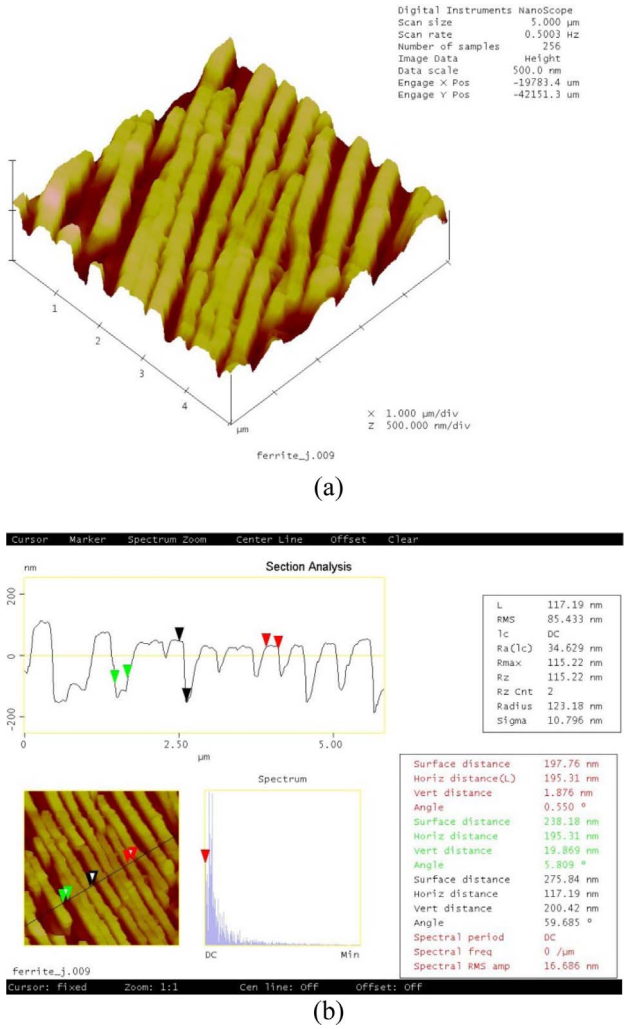

Fig. 8. (Color online) (a) AFM image of inter-lamellar microstructure in cross-section of carburized and heat treated Fe powder and (b) test line applied in a direction perpendicular to the inter-lamellar structure imaged by AFM (5 um × 5 um scale) and topographic profile corresponding to the region crossed by the test line.

Table 1. Measured average inter-lamellar spacing in the carburized and heat treated powder.

Every measured area	Average height (nm)	Average ferrite width (nm)	Average cementite width (nm)
5 um × 5 um	102.93 ± 11.3	387.66 ± 38.1	109.74 ± 17.2

SAD patterns prove that α-ferrite has BCC (110) plane distance and adjacent stoichiometric Fe_3C cementite has an orthorhombic crystal structure. The pattern has been indexed to the crystalline cementite with [102] crystal axis parallel to the electron beam. This structure is the same as a well-known pearlite structure in the plain-carbon steel field [13].

The properties of irons and steels are linked to the chemical composition, processing path, and resulting microstructure of the material. For a particular iron and steel composition, for example in this inter-lamellar structure, most properties depend on microstructure.

The topographic features revealed on AFM images, with cementite lamellae forming "hills" above ferrite "valleys", facilitate the choice of the nano-scale inter-lamellar spacing colonies apparently perpendicular to the sectioning plane, exhibiting microstructures such as the one shown in Fig. 8.

As observed in SEM & TEM images in Figs. 6 and 7, the 3-dimensional AFM images also present the topographic features of inter-lamellar microstructure having trench type hills and valleys. Mean true lamellar spacings such as ferrite and cementite width as well as average height can be calculated precisely as described in Table 1. The average height from ferrite bottom to the Fe_3C cementite top is 102.93 nm and the average width of α-ferrite is almost four times larger than that of Fe_3C cementite. These results are similar to the width measurement of TEM results. However, there are some deviations in some areas and the reason of this variation is ambiguous. We infer that the cooling rates, carbon contents, the degree of deformation, the amount of defects such as dislocations, vacancies can be one of the reasons. We need to scrutinize based on these reasonable possibilities.

A comparative analysis allows us to conclude about an identity of the information extracted by means of TEM and AFM techniques on the morphology of the products of the structure transformation taking place in Fe powders due to the carburization and heat treatment. So using AFM to control structural state of samples can make this procedure much easier and faster because of essential simplicity of AFM analysis compared to TEM analysis that requires the vacuum facilities. Moreover, AFM allows one to extract some information additional to the obtained by TEM. For example, it can be obtained more detailed information on structure and morphology of separate phase components of samples such as surface topography and phase contrast.

3.3. Magnetic properties

Based on the information about the microstructure of three kinds of powders, we can infer the mechanism how the microstructural constituents have an effects on the magnetic properties such as permeability, magnetic flux and core loss.

Fig. 9 shows the quality factor, Q as a function of applied frequency from 1 kHz to 100 MHz for the compacted polycrystalline Fe/SiO_2 composites, amorphous $Fe\text{-}Cr\text{-}Si\text{-}B/SiO_2$ composites and Fe/SiO_2 composites having an inter-lamellar microstructure. The Q of an inductor is

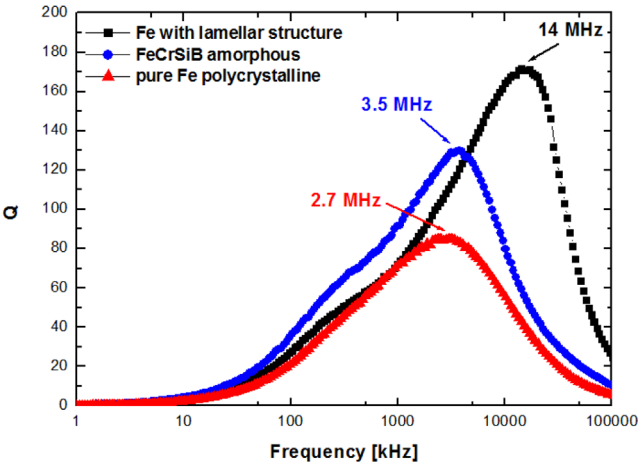

(a)

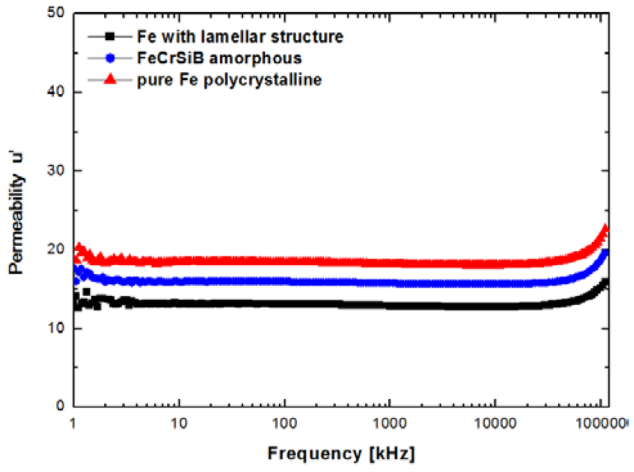

(b)

Fig. 9. (Color online) (a) The quality factor (Q) and (b) initial permeability (u') variation as a function of applied frequency.

Table 2. Packing density and ratio of toroid cores.

	Packing density [g/cc]	Packing ratio [%]
Fe with lamellar structure	4.86	62.6
FeCrSiB amorphous	4.73	65.7
Pure Fe polycrystalline	5.23	67.1

the ratio of its inductive reactance to its resistance at a given frequency, and is a measure of its efficiency. The higher the Q factor, the closer it approaches the behavior of an ideal, loss minimization and thus we need to increase the Q as much as possible.

In this experiment, we used all the powders having similar particle size distribution in order to exclude the effects of particle size on the intra & inter particle eddy current loss. In general, the core loss has a tendency to decrease as the particle size decreases, because the particle boundary area portion in core mass increases with decreasing particle size.

For the pure Fe polycrystalline, namely only α-Fe phase, the Q factor reaches its maximum value 85 at 2.7 MHz and then decreases as the frequency increases. In case of amorphous Fe, its Q maximum factor is located at 3.5 MHz and Q value is about 140 because its electrical resistivity is higher than polycrystalline Fe due to the difficulty of electron mobility. This means that amorphous structure has smaller eddy currents flow in the unit volume than polycrystalline structure. However, the drawback of amorphous Fe is lower Ms (magnetization) value than polycrystalline Fe due to its smaller Fe contents. This cause deteriorates the DC-bias characteristics of power inductor.

Our developed Fe/SiO_2 composite with lamellar structure shows the highest maximum Q factor at 14 MHz and Q value is 170. Dense and fine inter-lamellar Fe_3C cementite walls which are observed prevent the eddy current from flowing and merging in the powder matrix and then separate total eddy currents as the frequency increases. Moreover, the high Fe contents except 0.8% carbon contents which is necessary to make lamellar structure empirically, can contribute the high magnetization. This means our unique microstructure can provide both high DC-bias characteristics and small core loss property simultaneously.

As shown in Fig. 9(b) and Table 2, considering the permeability, the pure Fe polycrystalline composite core shows the highest value due to its highest packing ratio. This also can be due to the ductile property compared to the other powder cores. The permeability is strongly influenced by the packing ratio, and their stable permeability

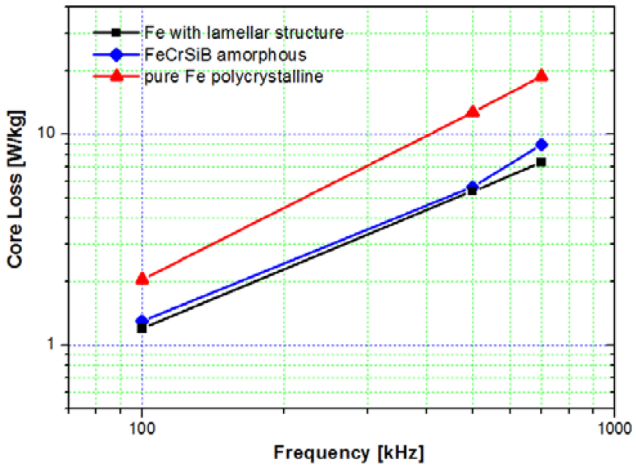

Fig. 10. (Color online) Core loss in variation with applied frequency. Intra-particle eddy current loss decrease drastically at all frequency range by structural modification.

values vary from 13 to 18 irrespective of frequency almost up to 60 MHz.

Apart from the quality factor, Q value measurement, the core loss measurement is also necessary to evaluate only the eddy current and hysteresis loss dominantly. Fig. 10 shows the core loss change as a function of the applied frequency to evaluate the materials efficiency. In this characterization, we change the test frequency 100, 500 and 700 kHz due to the packing density of toroid sample and consider the motor application fields. As the frequency increases from 100 kHz to 700 kHz, the core loss also increases linearly due to the eddy currents flow at all composite powders. The newly developed Fe/SiO_2 composites with inter-lamellar structure exhibits significantly reduced core loss compared with the conventional pure Fe polycrystalline/SiO_2 composites. Even compared to the amorphous Fe-Cr-Si-B/SiO_2 composites, the inter-lamellar structure powder composites show lower core loss at all frequencies.

Thus the newly developed composite powder having inter-lamellar microstructure is expected to be used for applications such as motors that rotate at relatively very high speed and frequency. Based on the microstructure that we have observed using SEM, TEM, STEM and AFM, it can be suggested that the area within which the eddy current flows can be separate minutely due to the nano-scale cementite block walls.

Considering the magnetic flux and DC-bias characteristics, magnetization (Ms) and coercivity (Hc) are also important factors in power inductor and motor applications.

Fig. 11 and Table 3 show the magnetization and coercivity variation to evaluate the materials DC magnetic property as the microstructure change. It is well recog-

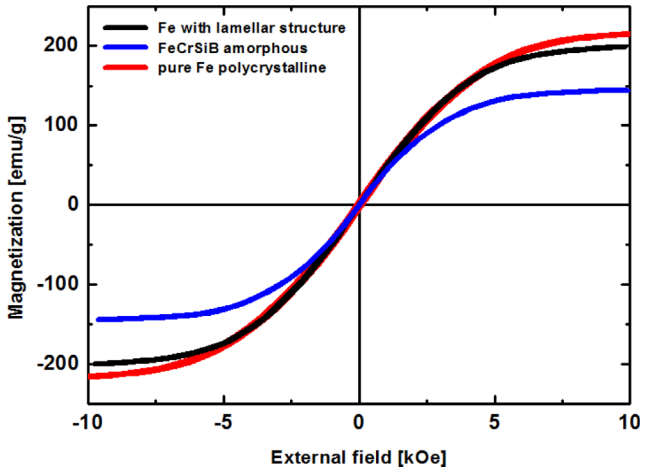

Fig. 11. (Color online) Magnetization (Ms) and coercivity (Hc) variation measured by vibrating sample magnetometer (VSM). These values are strongly affected by Fe contents and microstructure.

nized that as the magnetization increases as the Fe content increases and the hysteresis loss of a material corresponds to the looped area in the MH curve (magnetic flux density vs. magnetic field), in which the size of the loop correlates strongly with the material's coercive force, or coercivity [14].

As we have expected, the pure Fe polycrystalline powder shows the highest magnetization, 221 emu/g and coercivity 16 Oe, respectively. On the other hand, FeCrSiB amorphous powder decreases the coercivity down to 9 Oe due to the high electrical resistivity and smaller defects such as grain boundary, but also has the weak point of the lowest magnetization, 144 emu/g due to the small amount of Fe contents.

Our developed Fe/SiO_2 composite with lamellar structure, however, exhibits almost similar magnetization, 199 emu/g to the pure Fe and the smallest coercivity 4 Oe. This means that it can be achievable to obtain materials having both the high DC-bias and magnetic flux characteristics similar to the pure polycrystalline Fe, and relatively small eddy current loss almost equal to the amorphous Fe, as the maximum usable frequency increases. These dual merits, namely, can be achievable by only microstructure modification without losing Fe contents.

Table 3. Magnetization (Ms) and coercivity (Hc) value.

	Magnetization [emu/g]	Coercivity [Oe]
Fe with lamellar structure	199	4
FeCrSiB amorphous	144	9
Pure Fe polycrystalline	221	16

3.4. The effects of the inter-lamellar structure on the magnetic properties based on the skin depth

All the experimental results demonstrate that Fe metal composite with inter-lamellar structure indicate lower eddy current loss than pure Fe polycrystalline powder composite as the frequency increases up to the MHz range. At this point, we need to investigate why the inter-lamellar structure has influence on the magnetic properties and what is the limitation of α-ferrite and cementite width in relation to the skin depth. It is well noted that eddy currents are electrical currents induced within conductors like metals by changing magnetic fields and increase drastically at high frequencies [15-18]. These circulating eddies of current have inductance and thus induce magnetic fields. These fields can cause repulsive, drag and heating effects. The stronger the applied magnetic field, or the greater the electrical conductivity of the conductor, or the faster the field changes, then the greater the currents that are developed and the greater the repulsive fields produced. To minimize this kind of eddy current loss, the magnetic materials should be designed with thickness below the double skin depth. The skin effect is the tendency of an alternating electric current to become distributed within a conductor such that the current density is largest near the surface of the conductor, and decreases with greater depths in the conductor. At high frequencies, the skin depth becomes much smaller. The skin depth can be expressed as follows [19]:

$$\delta = \sqrt{\frac{\rho}{\pi f \mu}} \tag{1}$$

where δ is the skin depth, f is the frequency, and μ is the permeability. The calculated skin depth, resistivity, and related magnetic size such as average particle size and the width of α-ferrite in the inter-lamellar structure are shown in Table 4.

Based on the basic assumption that the particle is perfect sphere and has no defects such as dislocations, vacancies and grain boundaries, FeCrSiB amorphous indicate the

Table 4. Skin depth variation for the change of material's composition and microstructure.

Material	Magnetic size [um]	Resistivity [Ω·m]	Skin depth × 2 [um]	
			1 MHz	10 MHz
Pure Fe polycrystalline	5~10	9.61×10^{-10}	4.93	1.56
FeCrSiB amorphous	5~10	1.4×10^{-4}	168	53.28
Fe with lamellar structure	0.3~0.4	1.43×10^{-7}	6.95	2.19

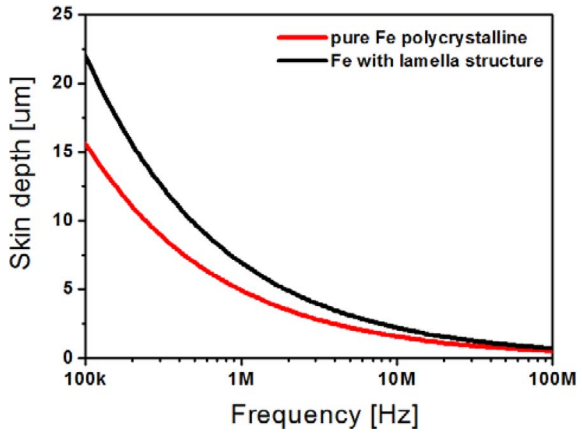

Fig. 12. (Color online) Frequency dependence of skin depth for the pure Fe and Fe composite with inter-lamellar microstructure.

largest skin depth due to the several order's higher resistivity than the other two iron materials. Theoretically, it can be used widely in the magnetic materials application fields in terms of the eddy current loss. However, due to the limitation of the 70~74% Fe contents to make amorphous structure, it cannot be used for high DC-bias characteristic inductor and high speed motor application that should possess high permeability and magnetic flux density.

As shown in Fig. 12, if we consider only the pure Fe polycrystalline and Fe with inter-lamellar microstructure, the skin depth decreases with frequency at all range and the Fe with lamellar structure has larger skin depth than pure Fe.

The interesting point is that the pure Fe with 5~10 um particle size shows almost the same value, 4.93 um at 1 MHz and this means the eddy current loss occurs at an initial stage theoretically. As the frequency increases above 1 MHz, this pure Fe powder composite cannot be used due to the rapid increase of eddy current loss. On the contrary, Fe with lamellar structure shows the skin depth still higher than the magnetic size even at 10 MHz. Although the particle size of Fe with lamellar structure is about 5~10 um, the magnetic phase, α-ferrite width is only 300~400 nm. From the experimental results and these calculation data, this plausible mechanism can be suggested that every cementite walls block the eddy current flow within the particle. Thus, we can use this powder even at 10 MHz.

4. Conclusion

In this paper, the preparation of a soft magnetic composite having inter-lamellar microstructure manufactured by consecutive plasma carburization-heat treatment, and their magnetic properties have been studied. It is regarded as a suitable soft magnetic composite for use in high performance power inductor and motor applications especially at high frequency above 10 MHz if we can control the lamellar width, height and area portion in the matrix precisely. High efficiency and low loss magnetic devices can be obtained provided inter-lamellar structure is formed by proper carbon diffusion and heat treatment procedure. We can also anticipate this microstructure and related manufacturing composite method can be easily applied to the mass production process of conventional power inductor, common mode filter, and high speed motor.

Acknowledgments

This work was supported by the Energy Efficiency & Resources of the Korea Institute of Energy Technology Evaluation and Planning (KETEP) grant funded by the Korea government Ministry of Knowledge Economy (20122010300041).

References

[1] Q. Zhu, L. Li, M. S. Masteller, and G. J. Corso Del, Appl. Phys. Lett. **69**, 3917 (1996).
[2] T. Sato, T. Iijima, M. Seki, and N. Inagaki, J. Magn. Magn. Mater. **65**, 252 (1987).
[3] A. Makino, IEEE Trans. Magn. **48**, 1331 (2012).
[4] H. Shokrollahi and K. Janghorban, Mater. Sci. Eng. B **134**, 41 (2006).
[5] A. H. Taghvaei, H. Shokrollahi, and K. Janghorban, J. Magnetism & Magnetic Mater. **321**, 3926 (2009).
[6] T. Sugama, L. E. Kukacka, N. Carciello, and J. Warren, J. Mater. Sci. **23**, 101 (1988).
[7] H. Honma, J. Mater. Sci. **29**, 949 (1994).
[8] Y. Sun, X. Y. Li, and T. Bell, Surf. Eng. **15**, 49 (1999).
[9] J. Youles, Powder Handling & Processing **15**, 132 (2003).
[10] http://www.optique-ingenieur.org/en/courses/OPI_ang_M05_ C02/co/Contenu_02.html Fundamentals of Semiconductor Physics.
[11] A. Makino, H. Men, T. Kubota, K. Yubuta, and A. Inoue, Mater. Trans. **50**, 204 (2009).
[12] N. Ridley, Metall. Trans. A **15**, 1019 (1984).
[13] J. R. Davis, Metals Handbook Desk Edition, 2nd ed., 153 (1998).
[14] H. Hojo, N. Akagi, T. Sawayama, and H. Mitani, Kobelco Tech. Review **30**, 30 (2011).
[15] R. M. Bozorth, Ferromagnetism. Van Nostrand, New York (1951) Ch. 3-8. (reprinted by IEEE Press, New York, 1993).
[16] C. W. Chen, Magnetism and Metallurgy of Soft Magnetic

Materials, Dover, New York (1986).
[17] A. Goldman, Handbook of Modern Ferromagnetic Materials, Kluwer Academic Publishers, Boston (1999) Ch. 12.
[18] X. T. Huo, University of Canterbury, Electrical and Computer Engineering, Maters Thesis (2009).
[19] http://en.wikipedia.org/wiki/skin_effect.